SAND REPORT

SAND2004-6110
Unlimited Release
Printed November, 2004

Final Report: LDRD Project 69162 Solution Behavior of PEO: the Ultimate Biocompatible Polymer

John G. Curro and Amalie L. Frischknecht

Prepared by
Sandia National Laboratories
Albuquerque, New Mexico 87185 and Livermore, California 94550

Sandia is a multiprogram laboratory operated by Sandia Corporation, a Lockheed Martin Company, for the United States Department of Energy under Contract DE-AC04-94AL85000.

Approved for public release; further dissemination unlimited.

Sandia National Laboratories

Issued by Sandia National Laboratories, operated for the United States Department of Energy by Sandia Corporation.

NOTICE: This report was prepared as an account of work sponsored by an agency of the United States Government. Neither the United States Government, nor any agency thereof, nor any of their employees, nor any of their contractors, subcontractors, or their employees, make any warranty, express or implied, or assume any legal liability or responsibility for the accuracy, completeness, or usefulness of any information, apparatus, product, or process disclosed, or represent that its use would not infringe privately owned rights. Reference herein to any specific commercial product, process, or service by trade name, trademark, manufacturer, or otherwise, does not necessarily constitute or imply its endorsement, recommendation, or favoring by the United States Government, any agency thereof, or any of their contractors or subcontractors. The views and opinions expressed herein do not necessarily state or reflect those of the United States Government, any agency thereof, or any of their contractors.

Printed in the United States of America. This report has been reproduced directly from the best available copy.

Available to DOE and DOE contractors from
U.S. Department of Energy
Office of Scientific and Technical Information
P.O. Box 62
Oak Ridge, TN 37831

Telephone: (865)576-8401
Facsimile: (865)576-5728
E-Mail: reports@adonis.osti.gov
Online ordering: http://www.doe.gov/bridge

Available to the public from
U.S. Department of Commerce
National Technical Information Service
5285 Port Royal Rd
Springfield, VA 22161

Telephone: (800)553-6847
Facsimile: (703)605-6900
E-Mail: orders@ntis.fedworld.gov
Online order: http://www.ntis.gov/ordering.htm

SAND 2004-6110
Unlimited Release
Printed November 2004

Final Report: LDRD Project 69162

Solution Behavior of PEO: the Ultimate Biocompatible Polymer

John G. Curro and Amalie L. Frischknecht

Sandia National Laboratories

P. O. Box 5800

Albuquerque, New Mexico 87185

Table of Contents

Introduction……... page 5

Part 1. The Structure of Poly(ethylene oxide) Liquids: Comparison of Integral Equation Theory with Molecular Dynamics Simulations and Neutron Scattering …… page 6

Part 2. Implementation of TIP4P in LAMMPS……... page 26

Part 3 The Effect of an Electric Field on the Phase Behavior of a Flory-Huggins Polymer Solution…… page 34

Introduction

Poly(ethylene oxide) (PEO) is the quintessential biocompatible polymer. Due to its ability to form hydrogen bonds, it is soluble in water, and yet is uncharged and relatively inert. It is being investigated for use in a wide range of biomedical and biotechnical applications, including the prevention of protein adhesion (biofouling), controlled drug delivery, and tissue scaffolds. PEO has also been proposed for use in novel polymer hydrogel nanocomposites with superior mechanical properties. However, the phase behavior of PEO in water is highly anomalous and is not addressed by current theories of polymer solutions. The effective interactions between PEO and water are very concentration dependent, unlike other polymer/solvent systems, due to water-water and water-PEO hydrogen bonds. An understanding of this anomalous behavior requires a careful examination of PEO liquids and solutions on the molecular level.

We performed massively parallel molecular dynamics simulations and self-consistent Polymer Reference Interaction Site Model (PRISM) calculations on PEO liquids. We also initiated MD studies on PEO/water solutions with and without an applied electric field. This work is summarized in three parts devoted to:

1. A comparison of MD simulations, theory and experiment on PEO liquids
2. The implementation of water potentials into the LAMMPS MD code
3. A theoretical analysis of the effect of an applied electric field on the phase diagram of polymer solutions.

Part 1

The Structure of Poly(ethylene oxide) Liquids: Comparison of Integral Equation Theory with Molecular Dynamics Simulations and Neutron Scattering

Abstract

Polymer reference interaction site model (PRISM) calculations and molecular dynamics (MD) simulations were carried out on poly(ethylene oxide) liquids using a force field of Smith, Jaffe, and Yoon. The intermolecular pair correlation functions and radius of gyration from theory were in very good agreement with MD simulations when the partial charges were turned off. When the charges were turned on, considerably more structure was seen in the intermolecular correlations obtained from MD simulation. Moreover, the radius of gyration increased by 38% due to electrostatic repulsions along the chain backbone. Because the partial charges greatly affect the structure, significant differences were seen between the PRISM calculations (without charges) and the wide angle neutron scattering measurements of Annis and coworkers for the total structure factor, and the hydrogen/hydrogen intermolecular correlation function.

I. Introduction

Poly(ethylene oxide) (PEO) is a water soluble polymer that has many important technological applications. It is widely used as a drag reducer[1] in the flow of water in pipes. It has also found applications as a polymer electrolyte[2]. Perhaps the most important applications of PEO are biological since PEO is biocompatible with human blood and tissue[3]. Because of its importance, PEO has been the subject of numerous theoretical[4-10] and simulation studies[11-17].

PEO displays a closed loop phase diagram with water as a result of hydrogen bonding. PEO in aqueous solution has been modeled with various mean field theories[4-9] to include the effect of hydrogen bonding. Using the associating fluid approach of Semenov and Rubinstein[10], Dormidontova[9] developed a mean field theory that treats both polymer/water and water/water hydrogen bonds. This theory predicts a closed loop phase diagram in good agreement with experiment.

Various force fields have been developed[12,13-18] for PEO based on quantum calculations and the structure of PEO liquids has been studied in several[12,14,15, 19-21] molecular dynamics (MD) simulations. Wide angle neutron scattering has been employed in two studies[20,21] to probe the packing of PEO liquids. Smith, Bedrov and coworkers[11] have performed MD simulations of PEO in aqueous solution. Muller-Plathe and van Gunsteren[16] performed simulations of PEO in the presence of lithium ions. Small angle[19] neutron scattering measurements have been carried out to investigate the structure and chain dimensions of PEO/LiI solutions.

In the present investigation we performed Polymer Reference Interaction Site Model (PRISM) calculations[22] and MD simulations on PEO liquids on an atomistically

realistic, explicit atom model using the force field of Smith, Jaffe, and Yoon[18] (SJY). The focus of this work was to test the agreement between theory, simulation, and experiment for the intermolecular pair correlation functions and structure factors. In previous investigations[23,24] theoretical calculations and MD simulations of poly(dimethyl siloxane) (PDMS) liquids were carried out using united atom and explicit atom force fields, with and without partial charges. Surprisingly, it was found that even though the partial charges were of moderate magnitude, they had only a minor effect on the liquid structure and chain dimensions of PDMS. In this investigation we also examined the effect of partial charges on the structure of PEO liquids. In the next section we briefly describe the application of self-consistent PRISM theory and MD simulation to PEO liquids. In Section III we compare theory and simulation in the absence of charge. We then use MD simulation to examine changes in liquid structure and chain dimensions when the partial charges in the SJY force field are turned on. Finally we compare our theoretical calculations to wide angle neutron scattering results of Annis and coworkers[20] for both the total structure factor and the intermolecular correlations between H atoms in PEO liquids.

II. Theory and Simulation

A. PRISM Theory

PRISM theory[22,25-28] is an extension to polymers of the *reference interaction site model*, or RISM theory, of Chandler and Andersen[29,30] for small molecule liquids. The theory has been discussed extensively[22,28] and will only briefly be discussed here as applied to PEO liquids. Within the reference interaction site model, interactions and correlations of macromolecules occur between spherically symmetric interaction sites.

For PEO there are three independent, overlapping sites: C, O, and H representing the atoms making up the PEO repeat unit [–CH_2-O-CH_2-]. Basically PRISM theory provides a link between the average intramolecular structure of a single macromolecule and the intermolecular packing in a bulk liquid. The intramolecular structure is characterized by the function

$$\hat{\omega}_{\alpha\beta}(k) = \frac{1}{N_\alpha} \sum_{i \in \alpha} \sum_{j \in \beta} \left\langle \frac{\sin kr_{ij}}{kr_{ij}} \right\rangle \tag{1}$$

where the caret denotes the Fourier transform with wave vector k. For PEO α and β represent a C, O, or H site, and N_α represents the number of sites of type α on a chain. The brackets denote an average over a single chain, which we carry out using a single chain Monte Carlo simulation. The intermolecular packing of PEO is characterized by the six independent radial distribution functions $g_{\alpha\beta}(r)$ between sites α and β on *different* chains.

The generalized Ornstein-Zernike equation proposed by Chandler and Andersen[22,29,30] relates the intramolecular and intermolecular structure

$$\hat{\mathbf{H}}(k) = \hat{\boldsymbol{\omega}}(k) \cdot \hat{\mathbf{C}}(k) \cdot [\hat{\boldsymbol{\omega}}(k) + \hat{\mathbf{H}}(k)] \tag{2}$$

where the total correlation function is defined as

$$H_{\alpha\beta}(r) = \rho_\alpha \rho_\beta \left[g_{\alpha\beta}(r) - 1 \right] \tag{3}$$

and ρ_α is density of atoms of type α. The generalized Ornstein-Zernike equation can be viewed as a definition of the six direct correlation functions $C_{\alpha\beta}(r)$. In this work we approximate these direct correlation functions using the Percus-Yevick closure[22,31]

$$C_{\alpha\beta}(r) = \{1 - \exp[\beta V_{\alpha\beta}^{rep}(r)]\}[H_{\alpha\beta}(r) + 1] \tag{4}$$

which is known to be accurate for polymer liquids with strong repulsions and weak attractions at high density. Previous work[22] demonstrated that PRISM theory and the Percus-Yevick closure works best for repulsive potentials. Hence in eq 4 we employ only the repulsive part of the potential $V^{rep}_{\alpha\beta}(r)$. This approximation makes use of the well known fact that the structure of a van der Waals liquid is determined primarily by the repulsive component of the pair potential for liquids at high density. However, for liquids with partial charges, the electrostatic interactions may, depending on the magnitude of the charges, influence the pair correlations. We will investigate this question later in this paper.

The SJY force field[18] represents the nonbonded interactions with an exponential-6 and Coulombic potential of the form

$$
\begin{aligned}
V_{\alpha\beta}(r) &= V_{\alpha\beta}(r^*), \quad r \le r^* \\
&= \left(\frac{6}{\alpha-6}\right)\exp\left[\alpha\left(1-(r/R_0)\right)\right]\left(\frac{\alpha}{\alpha-6}\right)\left(\frac{R_0}{r}\right)^6 + K_c\frac{q_\alpha q_\beta}{r}, \quad r > r^*
\end{aligned}
\tag{5}
$$

where K_c=332.08 when the charges are turned on. The exp-6 potential in eq 5 is non-monotonic in the repulsive regime and has a maximum at a separation r*. In the MD simulations, separations r<r* are never accessed and this cutoff is not relevant since $V(r^*)/k_BT$ is very large for the PEO model studied here. However in our PRISM calculations, single chain Monte Carlo simulations using the pivot algorithm[33] are employed and it is important to apply a cutoff r* at short distances so that no two atoms overlap. The parameters for PEO are given in Tables 1 and 2 based on the SJY[18] force field. In eq 4 for the closure we use only the repulsive branch of the exp-6 potential defined analogously to the method of Weeks, Chandler, and Andersen[32] for the Lennard-Jones potential.

$$
\begin{aligned}
V^{rep}_{\alpha\beta}(r) &= V^{rep}_{\alpha\beta}(r^*) + \lambda, \quad r \le r^* \\
&= V^{rep}_{\alpha\beta}(r) + \lambda, \quad r^* \le r \le R_0 \\
&= 0, \quad r \ge R_0
\end{aligned}
\tag{6}
$$

In our PRISM calculations the charges are turned off (K_c=0).

Table 1. Nonbonded exp-6 parameters for PEO from SJY[18].

atom pair ($\alpha\beta$)	**ε(kcal/mol)**	**R_0 ($d^{\dagger}$) (Angstroms)**	**α**
CC	0.094813	3.8719 (3.10)	11.964
CH	0.051988	3.2741 (2.47)	11.181
HH	0.0098036	3.3698 (2.25)	12.603
CO	0.15257	3.4566 (2.88)	12.364
HO	0.044729	3.2778 (2.53)	12.790
OO	0.20334	3.1991 (2.54)	12.998

† The effective hard core diameter d was computed from eqs 5, 6, 11.

Table 2. Partial atomic charges from the SJY[18] force field

atom (α)	**q_α**
C	-0.066
H	0.097
O	-0.256

Because PEO is a flexible macromolecule, one would anticipate that the intramolecular and intermolecular parts of the problem are coupled, requiring that $\Delta_{\alpha\beta}(r)$

and $g_{\alpha\beta}(r)$ be determined in a self-consistent manner[22,33]. To carry out this iterative scheme, we employ a solvation potential $W_{\alpha\beta}(r)$ acting on a single chain during our Monte Carlo calculation. The purpose of this solvation potential is to mimic the effects of the other chains in the system. Assuming pairwise additivity, $\hat{W}_{\alpha\beta}(k)$ (in Fourier transform space) can be approximately calculated[22,34,35] from

$$\beta\hat{W}_{\alpha\beta}(k) \approx \sum_{i,j} \hat{C}_{\alpha i}(k)\hat{S}_{ij}(k)\hat{C}_{j\beta}(k) \tag{7}$$

where the structure factors are defined according to

$$\hat{S}_{\alpha\beta}(k) = \delta_{\alpha\beta} + \hat{H}_{\alpha\beta}(k) \tag{8}$$

Thus in our single-chain Monte Carlo simulation, the chain is subject to the pair potential $v_{\alpha\beta}(r)$ consisting of the bare, excluded volume repulsive potential of eq 6, and the attractive solvation potential in eq 7 due to the other chains.

$$v_{\alpha\beta}(r) = V^{rep}_{\alpha\beta}(r) + W_{\alpha\beta}(r) \tag{9}$$

A first approximation is to make use of the *Flory ideality assumption*[36] which assumes that these two contributions approximately cancel each other out so that a chain in a melt is ideal. A more quantitative treatment, which we follow here, requires us to carry out the full self-consistent computation in the following manner: We first guess the solvation potential and use this in a single-chain Monte Carlo simulation[33] to calculate $\hat{\omega}_{\alpha\beta}(k)$. With $\hat{\omega}_{\alpha\beta}(k)$, we use eqs 2 and 4 to solve for $\hat{H}_{\alpha\beta}(k)$ and $\hat{C}_{\alpha\beta}(k)$. This then allows us to calculate a new solvation potential with eq 7, and we continue to iterate until the difference between the new and old solvation potentials becomes very small. It should be mentioned that it is not necessary to perform a new Monte Carlo simulation with each

iteration. Reweighting techniques[33] can be used to greatly reduce the number of simulations that need to be carried out during the course of the self-consistent calculation.

When we carry out the single-chain Monte Carlo simulation, as well as, our full MD simulations we use the intramolecular potentials from the SJY force field. The bond stretching and bending potentials are taken to be harmonic

$$V_b = \frac{1}{2} k_b (r - r_0)^2 \tag{10a}$$

$$V_\theta = \frac{1}{2} k_\theta (\theta - \theta_0)^2 \tag{10b}$$

and the parameters were taken from reference 18. Our torsional potentials have the form

$$V_t = \sum_{i=0}^{3} a_i \cos^i(\phi) \tag{10c}$$

and the torsional parameters were extracted from the SJY force field[18] and are listed in Table 3.

Table 3. Torsional parameters (kcal/mol) in eq 10c extracted from the SJY force field[18]

torsional angles	$\mathbf{a_0}$	$\mathbf{a_1}$	$\mathbf{a_2}$	$\mathbf{a_3}$
HCOC	0	-1.215	0	1.620
COCO	0.350	0.020	-0.070	0.640
OCCH	0	-0.420	0	0.560
OCCO	1.275	0.025	-2.550	0

B. MD Simulations

The simulations were carried out using the LAMMPS parallel MD code[37] on systems containing chains of 105 atoms. Overlapping initial configurations were prepared from randomly placed chains with configurations chosen from the Monte Carlo simulations in our PRISM calculations. The overlaps were then removed by *pushing off*

with a soft nonbonded potential. A time step of 0.04 fs was used with a multiple time step integrator (RESPA) so that forces were calculated for every time step for bonded interactions, every two time steps for three and four body interactions, and every four time steps for exp-6 and Coulombic interactions. The long range Coulombic forces were calculated with a particle – particle/particle – mesh Ewald algorithm[38]. The simulations were run at constant density of $0.1010/A^3$ and the temperature was controlled with a Nose-Hoover thermostat using a coupling frequency of $0.02\ fs^{-1}$.

III. Results and Discussion

Self-consistent PRISM calculations were carried out for PEO liquids at 318K consisting of chains of 15 monomers (105 atoms) at a density of $0.1010\ atoms/A^3$. The partial charges were turned off and only the repulsive branch of the exp-6 potential was used in the PY closure. MD simulations were also performed on this same system using the full exp-6 potential of eq 5 (K_c=0). Six independent intermolecular radial distribution functions between CC, HH, OO, CO, OH, and CH pairs of sites are needed to completely characterize the packing.

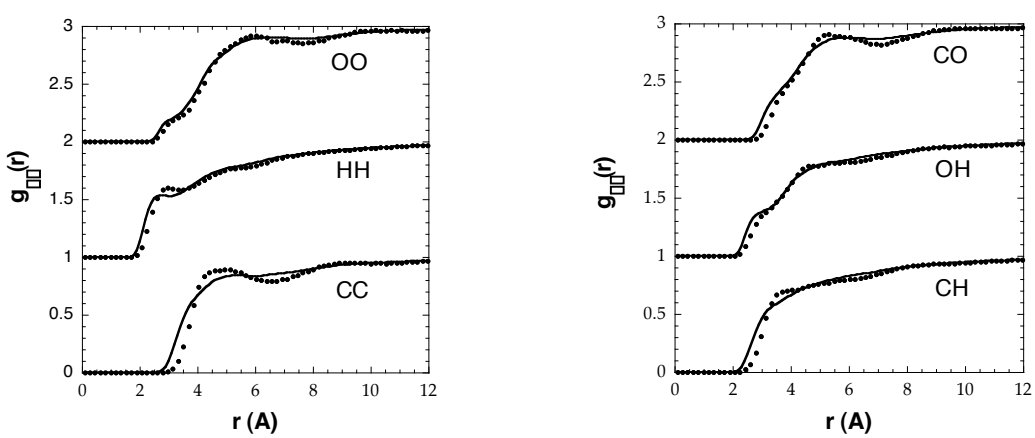

Figs. 1 and 2. *Intermolecular radial distributions functions for PEO (N=15) in the liquid state at 318°K and density 0.1010atoms/A³. Partial charges were turned off. Points – MD simulation, solid curves – PRISM theory. The curves are shifted along the y-axis for clarity.*

Figures 1 and 2 show a comparison between the PRISM theory and the MD simulation for these radial distribution functions. It can be seen that the agreement between theory and simulation is very good when there are no Coulombic interactions.

We can estimate the effective hard core distance $d_{\alpha\beta}$ between the various pairs of intermolecular sites from the Barker-Henderson formula[31]

$$d_{\alpha\beta} = \int_0^{\infty} \left[1 - \exp(-\beta V_{\alpha\beta}^{rep})\right] dr \qquad (11)$$

where we use the repulsive exp-6 potential defined in eqs 5 and 6. Based on the SJY parameters, the various $d_{\alpha\beta}$ are shown in Table 1. Examination of Figures 1 and 2 reveal that all the pair correlations $g_{\alpha\beta}(r)$ start to become nonzero at distances near $d_{\alpha\beta}$. This indicates that the backbone sites can come into contact with each other and are not completely screened out by the pendant hydrogen atoms.

Note that in the case of $g_{CC}(r)$ the theory predicts somewhat less structure than seen in the simulations. This is consistent with previous work[39] on an explicit atom model for polyethylene (PE) liquids and reflects the fact that PRISM theory is least accurate in predicting correlations between backbone sites that are shielded, in this case by the attached hydrogen atoms. It is instructive to directly compare the CC, HH, and CH intermolecular correlation functions in PEO liquids with polyethylene liquids shown in Figure 3. As can be seen the packing in PEO and PE melts is very similar, although more structure is seen in the PE g(r)'s. This is likely due to the greater flexibility of the PEO chain backbone that permits a wider range of intermolecular contacts and fewer preferred intermolecular distances.

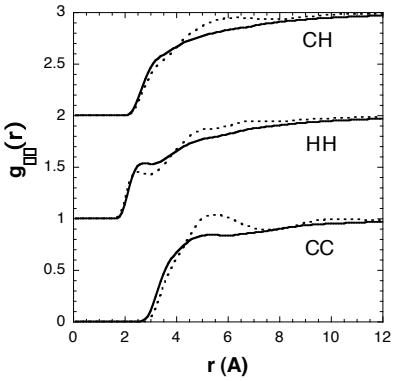

Fig. 3. *Intermolecular pair correlation functions associated with C and H obtained from PRISM theory. Solid curves – PEO, N=15, T=318K. Dotted curves –* $C_{20}H_{40}$ *from reference 39. The curves are shifted along the y-axis for clarity.*

We have demonstrated that PRISM theory gives good agreement with MD simulations of PEO liquids when the Coulombic interactions are turned off. We now examine the effect of partial charges on the liquid packing. MD simulations were performed using the charges from the SJY potential given in Table 2. A comparison of the radial distribution functions with and without charges is given in Figures 4 and 5. It can be seen that significantly more structure develops in pair correlations involving oxygen and carbon as a result of the charges. The partial charges also have a dramatic effect on the root-mean-square radius of gyration R_g. In Table 4 good agreement is seen in the R_g from MD and PRISM when the charges are turned off.

Table 4

	MD (full)	MD (no charge)	PRISM
R_g (A)	9.91 ± 0.07	7.37 ± 0.10	7.6

However, when the charges are turned on the PEO chains significantly expand and R_g increases by 38%. Because the chains are more extended, additional intermolecular overlap is allowed between PEO macromolecules leading to the additional structure in the intermolecular radial distribution functions seen in Figures 4 and 5.

The dramatic increase in R_g due to the charges presumably arises from long-range, Coulombic repulsions between like charges along the PEO chain backbone. From Table 2 it can be seen that the both the C and O backbone atoms are negatively charged whereas

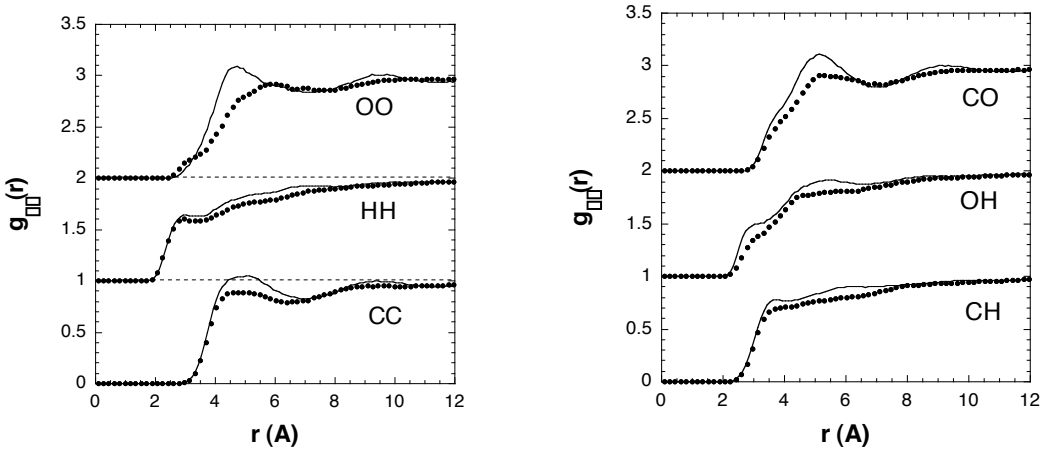

Figs. 4 and 5. *PEO Intermolecular radial distribution functions obtained from MD simulation. N=15, T= 318°K, and density= 0.1010atoms/A³. Points – without charges, solid curves – with charges. The curves are shifted along the y-axis for clarity.*

the pendant hydrogens are positively charged to preserve neutrality. We can compute the intermolecular charge density about each of these atoms from the relation

$$\rho_{e\alpha}(r) = \sum_{\beta} q_{\beta} g_{\alpha\beta}(r) \qquad (12)$$

Results are shown in Figure 6 based on the MD simulations. As can be seen the charge density is oscillatory with each atom on a given chain surrounded by positive charge in the 2.5 – 3.2 A regime due to the H atoms from other chains. The charge density changes

to negative in the 5 A region due to intermolecular C and O atoms. Finally the charge density decays to zero on 10 –15 A length scale. In a recent study[24] on PDMS liquids, we

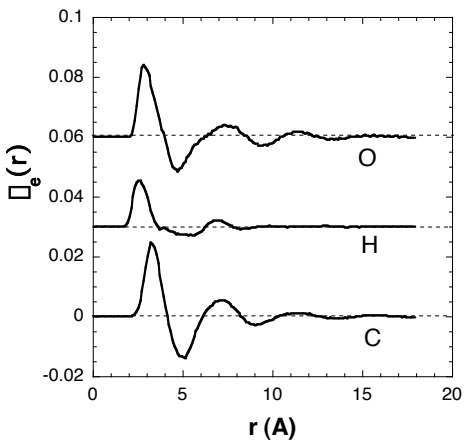

Fig. 6. *The intermolecular charge distribution around each atom in PEO calculated from eq 12. The curves are shifted along the y-axis for clarity.*

found that the partial charges had a smaller effect on R_g and the intermolecular pair correlation functions, even though the magnitude of the charges is similar in the two macromolecules. However in PEO each backbone C or O site is negatively charged, whereas in PDMS the Si and O atoms along the backbone are positive and negative respectively.

Wide angle neutron scattering has been used to study the structure of fully deuterated PEO liquids by two groups[20,21]. In Figure 7 we show the structure factor H(k) of PEO at 363K reported by Annis et al[20] defined according to

$$H(k) = \frac{I(k) - S_{self}}{\left[\sum_{\alpha} x_{\alpha} b_{\alpha}\right]^2} \qquad (13)$$

where x_{α} and b_{α} are the atomic fraction and coherent neutron scattering length of atoms of type α in a monomer. In eq 13 the self-scattering $S_{self} = \sum_{\alpha} x_{\alpha} b_{\alpha}^2$ is subtracted from the total differential neutron scattering cross section per atom I(k). The factor in the

denominator normalizes the scattering to a monomer basis. The coherent scattering lengths for C and O in natural abundance, and H^2 were taken from reference 40.

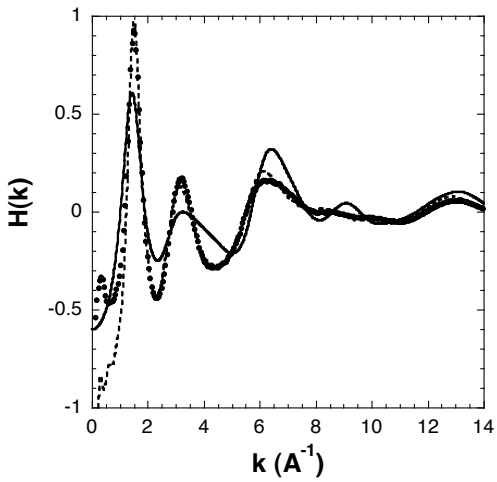

Fig. 7. *The total structure function H(k) defined in eq 13 for PEO liquid at 363°K. Points are from the wide angle neutron diffraction experiments of Annis et al[20]. Solid curve – PRISM theory (N=54, T=363°K) with charges off. Dashed curve – MD simulations from reference 20 (N=54, T=363°K) with charges on.*

We performed self-consistent PRISM calculations for PEO liquids of 54 monomers at T=363K at the experimental density of 0.103 atoms/A^3. As before, the charges were turned off in the PRISM calculation. The scattering intensity I(k) was calculated from

$$I(k) = \sum_{\alpha\beta} x_\alpha b_\alpha b_\beta \hat{S}_{\alpha\beta}(k) / \Omega_\alpha \qquad (14)$$

using the partial structure factors defined in eq 8. Eq 13 was then employed to obtain an estimate of H(k). A comparison of PRISM theory with the neutron scattering experiments is shown in Figure 7. The differences between theory and experiment are due to inaccuracies of the theory and the SJY potentials, but are primarily due to the effect of omitting the partial charges in the PRISM calculation. Also shown in Figure 7 are MD simulations reported in reference 20 using the full SJY force field. Note that as in the case of the g(r)'s in Figures 4 and 5, the inclusion of charges in the MD simulation leads to additional structure in H(k) relative to the theory. Refinements were made to the SJY

force field by Borodin et al in a later study[12] which, when used in an MD simulation[12] of PEO liquids, is in quantitative agreement with the neutron scattering measurements[20] of Annis et al.

A useful feature of wide angle neutron scattering[41,41,20] is that the pair correlation function $g_{HH}(r)$ between the hydrogen atoms can be directly extracted from experiments on hydrogenated and deuterated samples. Previously, both PRISM theory[39] and MD simulations were compared with experimental[41,42] $g_{HH}(r)$ for polyethylene and alkane liquids. Here we make a similar comparison with the data of Annis[20] for PEO liquids. This comparison is shown in Figure 8 as the Fourier transform of the total correlation function

$$h_{HH}(r) = g_{HH}(r) - 1 \tag{15}$$

As in the case of the total structure factor H(k), we likewise see that PRISM theory predicts less structure than experiment for the HH correlations.

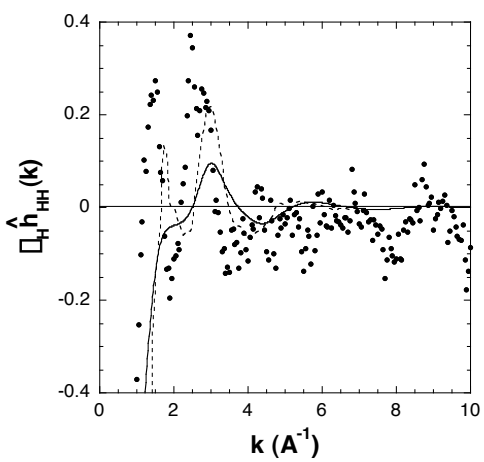

Fig. 8. *The HH pair correlation function defined in eq 15 (in Fourier space) for PEO liquid at 363°K. Points are from the wide angle neutron diffraction experiments of Annis et al[20]. Solid curve – PRISM theory (N=54, T=363°K) with charges off. Dashed curve – MD simulations from reference 20 (N=54, T=363°K) with charges on.*

Also shown in Figure 8 is the MD simulation reported in reference 20 with the full SJY force field. In view of our earlier results it is not surprising that PRISM theory, with no charges, also predicts less structure in $\hat{h}_{HH}(r)$than the MD simulation with charges.

IV. Conclusions

Our main finding in this study is that the partial charges surrounding the atoms have a significant effect on the chain dimensions and intermolecular packing in poly(ethylene oxide) liquids. This effect is not seen in poly(dimethyl siloxane) liquids even though the magnitude of the charges in the two systems are comparable. The different responses may be related to the fact that in PEO all atoms on the chain backbone are negatively charged and the intramolecular Coulombic repulsions may be long range. In the case of PDMS, the backbone atoms alternate in the sign of the charge which may cause the Coulombic repulsions to be screened to a larger degree than in PEO. Since the individual chains become extended as a result of the charges, there is more intermolecular overlapping of chains in the liquid, which is reflected in more structure in the corresponding intermolecular radial distribution functions.

In PEO liquids without partial charges, there is very good agreement between self-consistent PRISM theory and MD simulations. PRISM theory, when used with the Percus-Yevick closure of eq 4, is most accurate for macromolecular liquids with strong repulsions and weak attractions. Hence this PRISM/PY approach is probably not appropriate for describing macromolecular liquids with strong Coulombic interactions. Other *molecular closures*[22,43] have been used successfully in describing the effect of attractions on liquid structure. Another approach using PRISM theory, which is beyond

the scope of this investigation, is to include the full Coulombic interactions in the single chain simulation part of the self-consistent calculation but retaining the repulsive PY closure.

References

1. Lumley, J. L.; *Ann. Rev. Fluid Mech.* **1969**, 1, 367.
2. Gray, F. M.; *Polymer Electrolytes*; Royal Soc. of Chemistry: Cambridge, 1997.
3. Harris, J. M. Ed. *Poly(ethylene glycol) Chemistry: Biotechnical and Biomedical Applications*; Plenum Press: New York, 1992.
4. Karlstrom, G. *J. Phys. Chem.* **1985**, 89, 4962.
5. Linse, P. *Macromolecules* **1993**, 26, 4437.
6. de Gennes, P. G. *C. R. Acad. Sci. Paris II* **1991**, 117, 313.
7. Matsuyama, A.; Tanaka, F. *Phys. Rev. Lett.* **1990**, 65, 341.
8. Bekiranov, S; Bruinsma, R.; Pincus, P. *Phys. Rev. E* **1997**, 55, 577.
9. Dormidontova, E. E. *Macromolecules* **2002**, 35, 987.
10. Semenov, A. N.; Rubinstein, M. *Macromolecules* **1998**, 31, 1373.
11. Smith, G. D.; Bedrov, D. *J. Phys. Chem. A* **2001**, 105, 1283. *J. Phys. Chem. B* **2003**, 107, 3095.
12. Borodin, O.; Douglas, R.; Smith, G. D.; Trouw, F.; Petrucci, S. *J. Phys. Chem. B* **2003**, 107, 6813.
13. Smith, G. D.; Borodin, O.; Bedrov, D. *J. Comp. Chem.* **2002**, 23, 1480.
14. Bin, L.; Boinske, P. T.; Halley, J. W. *J. Chem. Phys.* **1996**, 105, 1668.
15. Halley, J. W.; Duan, Y.; Nielsen, B.; Redfern, P. C.; Curtiss, L. A. J. Chem. Phys. **2001**, 115, 3957.
16. Muller-Plathe, F.; van Gunsteren, W. F. *J. Chem. Phys.* **1995**, 103, 4745.
17. Hyun, J. K.; Dong, H.; Rhodes, C. P.; Frech, R.; Wheeler, R. A. *J. Phys. Chem. B* **2001**, 105, 3329.

18. Smith, G. D.; Jaffe, R. L.; Yoon, D. Y. *J. Phys. Chem.* **1993**, 97, 12752.

19. Annis, B. K.; Kim, M.; Wignall, D. D.; Borodin, O.; Smith, G. D. *Macromolecules* **2000**, 33, 7544.

20. Annis, B. K.; Borodin, O.; Smith, G. D.; Benmore, C. J.; Soper, A. K.; Londono, J. D. *J. Chem. Phys.* **2001**, 115, 10998.

21. Johnson, J. A.; Saboungi, D. L.; Price, D. L.; Ansell, S.; Russell, T. P.; Halley, J. W.; Nielsen, B. *J. Chem. Phys.* **1998**, 109, 7005.

22. Schweizer, K. S.; Curro, J. G. *Adv. Chem. Phys.* 1997, *98*, 1.

23. Sides, S. W.; Curro, J. G.; Grest, G. S.; Stevens, M. J.; Soddemann, T.; Habenschuss, A.; Londono, J. D. *Macromolecules* **2002**, 35, 6455.

24. Frischknecht, A. L.; Curro, J. G.; *Macromolecules* **2003**, 36, 2122.

25. Schweizer, K. S.; Curro, J. G. *Phys. Rev. Lett.* **1987**, *58*, 246.

26. Curro, J. G.; Schweizer, K. S. *Macromolecules* **1987**, *20*, 1928.

27. Curro, J. G.; Schweizer, K. S. *J. Chem. Phys.* **1987**, *87*, 1842.

28. Heine, D. R.; Grest, G. S.; Curro, J. G. *Adv. Polym. Sci.* **2004**, in press.

29. Chandler, D.; Andersen, H. C. *J. Chem. Phys.* **1972**, *57*, 1930.

30. Chandler, D. in Montroll, E. W.; Lebowitz, J. L. Eds.; *Studies in Statistical Mechanics VIII*; North-Holland: Amsterdam, 1982.

31. Hansen; J. P.; McDonald, I. R. *Theory of Simple Liquids*; Academic Press: London, 1986.

32. Weeks, J. D.; Chandler, D.; Andersen, H. C. *J. Chem. Phys.* **1971**, *54*, 5237.

33. Pü tz, M.; Curro, J. G.; Grest, G. S. *J. Chem. Phys.* **2001**, *114*, 2847.

34. Chandler, D.; Singh, Y.; Richardson, D. M. *J. Chem. Phys.* **1984**, *81*, 1975.

35. Nichols, A. L.; Chandler, D.; Singh, Y.; Richardson, D. M. *J. Chem. Phys.* **1984**, *81*, 5109.

36 Flory, P. J., *J. Chem. Phys.* 1949, 17, 203.

37. Plimption, S. J.; *J. Comput. Phys.* **1995**, 117, 1.

38. Hockney, R.; Eastwood, J. *Computer Simulations Using Particles*; Adam Hilger: New York, 1988.

39. Tsige, M; Curro, J. G.; Grest, G. S.; McCoy, J. D. *Macromolecules* **2003**, 36, 2158.

40. *Neutron News* **1992**, 3, 29. http://www.ncnr.nist.gov/resources/n-lengths/list.html.

41. Londono, J. D.; Annis, B. K.; Turner, J. Z.; Soper, A. K. *J. Chem. Phys.* **1994**, *101*, 7868.

42. Londono, J. D.; Annis, B. K.; Habenschuss, A.; Smith, G. D.; Borodin, O.; Tso, C.; Hsieh; Soper, A. K. *J. Chem. Phys.* **1999**, *110*, 8786.

43. Schweizer, K. S.; Yethiraj, A. *J. Chem. Phys.* **1993**, 98, 9053.

Part 2

Implementation of TIP4P in LAMMPS

Amalie L. Frischknecht

This part summarizes the implementation of the TIP4P water potential into the parallel molecular dynamics code LAMMPS (Fortran90 version 2001), developed by Steve Plimpton.

The model

The TIP4P potential is for a 4-site water model, in which the charge due to the oxygen atom is displaced off of the oxygen atom by a small amount[1]. The whole molecule is held rigid, with OH bond lengths of 0.9572 Å and a fixed HOH angle of 104.52°. The fourth site, denoted M, is located a distance of 0.15 Å from the O atom along the bisector of the HOH angle. The intermolecular potential consists of two energetic terms, a single Lennard-Jones interaction between oxygen atoms and Coulomb interactions between all species:

$$U = \sum_i \sum_j \frac{q_i q_j e^2}{r_{ij}} + \frac{A}{r_{OO}} - \frac{C}{r_{OO}^6} \tag{1}$$

where A = 600.0 10^3 kcal $Å^{12}$/mol, C = 610.0 kcal $Å^6$/mol, r_{ij} is the distance between atoms *i* and *j* and r_{OO} is the oxygen-oxygen distance. The charges are given by q_O= 0, q_H = 0.52, q_M = -1.04.

Implementation in LAMMPS

This water model can be implemented in various ways. First, one could explicitly use 4 sites by introducing a fourth dummy atom M with a small mass. Holding the molecule rigid then requires an out-of-plane constraint. Since these kinds of constraints are not currently implemented in the SHAKE routines for LAMMPS, we did not pursue this option.

The second option is to only include the three real atoms in the dynamics and input files. Then, each time the forces are computed for a water oxygen atom, it is necessary to find the site M and compute the appropriate electrostatic interactions. A few new routines were added to force.f to calculate the appropriate forces. The basic idea is as follows. As the code runs through the neighbor list, if either atom *i* or atom *j* is a water oxygen, then we first find the location of site *M*; calculate the Coulomb force between site M and the other atom in the pair; and then redistribute the calculated force to the water oxygen and its attached hydrogen atoms. The redistribution of the force is found using equations from work by Feenstra et al[2]. Let $\mathbf{r}_O$, $\mathbf{r}_1$, and $\mathbf{r}_2$ be the position vectors of the oxygen and two hydrogen atoms in a given water molecule. Then the position of site *M* is given by

$$\mathbf{r}_M = \mathbf{r}_O + b\frac{\mathbf{r}_{O1} + 0.5\mathbf{r}_{12}}{|\mathbf{r}_{O1} + 0.5\mathbf{r}_{12}|} \tag{2}$$

where $\mathbf{r}_{O1} = \mathbf{r}_1 - \mathbf{r}_O$, $\mathbf{r}_{12} = \mathbf{r}_2 - \mathbf{r}_1$, and *b* is the bond length between site *M* and the O atom. The force acting on any given atom *i* due to the force on the dummy atom *M* can then be calculated from the partial derivative of the position of site *M* with respect to the position of atom *i*, as given by eq (6) in Feenstra et al.:

$$\mathbf{F}_{ix} = -\frac{\partial \mathbf{r}_M}{\partial x_i} \cdot \frac{\partial U}{\partial \mathbf{r}_M} = \frac{\partial \mathbf{r}_M}{\partial x_i} \cdot \mathbf{F}_M$$

where $\mathbf{F}_M$ is the force on site *M*. The redistributed forces on the various atoms are thus found from these two equations; the detailed formulas are given in eq (8) of Feenstra et al. with $a = 0.5$.

To implement this in LAMMPS, I modified the usual Lennard-Jones with the long-range Coulomb forces routine by creating a new force routine in force.f (called exp6_coul_long since this routine includes the entire PEO/TIP4P force field, for simulating PEO/water solutions). There are two requirements to using the implemented version. First, the routine is set up to work with Newton's third law turned on for the nonbonded forces, as will be explained below. Second, we assume that the water atoms have been entered sequentially by molecule in the initial LAMMPS input file, i.e. O1, H11,H12, O2, H21, H22, etc. The exp6_coul_long routine loops over all atom pairs in the neighbor list for each processor in order to calculate the nonbonded forces. We calculate Lennard-Jones-like forces first, in the usual way. Then, to calculate the Coulomb interactions, we use the following algorithm:

1. If atom *i* or *j* in the neighbor pair is a water oxygen atom, go to the find M subroutine to find the location of site *M*. This subroutine locates the local tags for the H atoms that are bonded to the O atom in question. This procedure requires that the atoms be entered sequentially as described above. The subroutine calculates the coordinates of site M and returns them.

2. Calculate the distance between site M and the other atom in the pair (possibly another site M on a different molecule).
3. Calculate the Coulomb force in the usual way; here we use the pppm version.
4. Add the forces appropriately in the force arrays. First, if atom *i* or atom *j* is a water oxygen atom, the force due to site M is distributed to the O atom to which it is bonded. Forces are also distributed to the other atom in the i,j pair (using Newton's third law).
5. Finally, if atom i or j is an H atom, we figure out what force to distribute to the H atom due to interactions between the M site assoicated with that H's water molecule and the other atom in the i,j pair. To do so, we go to the subroutine findM_H to find the O atom associated with this particular H atom. The subroutine returns the coordinates of site M, along with the atom tag of the O atom. We again calculate the Coulomb force between site M and the other atom in the force pair, and then distribute this force to the H atom in question.

The clearest way to calculate the virial for TIP4P is to use the formula

$$\frac{1}{3}\sum_i \mathbf{r}_i \cdot \mathbf{F}_i \tag{3}$$

summed over all atoms. LAMMPS calculates the virial this way when using Newton's third law for the nonbonded forces. It is then necessary to do step 5 as a separate step in order to correctly calculate the virial using this formula. This is due to the way LAMMPS handles "ghost" atoms which are outside the box owned by a particular processor. Basically, in calculating the virial the sum over atoms is done over both normal and ghost atoms. When we redistribute forces to the H atoms, we must make sure

that the force is stored in the correct copy of the H atom for the given processor, so that the force is then added correctly in the virial. Since the number of copies of an atom varies depending on the number of nodes used and the cutoffs, the way to ensure we get the right copy is to only make additions to the force array for atoms currently being looped over. Thus, even though we calculate the forces between site M and some other site in steps 2 and 3, the atoms in the i,j loop at that point that go with site M are oxygen atoms, not H atoms. If we distribute the force to the H atoms at the same time as to the O atoms in step 4, the forces and thus the dynamics will be correct but the virial will be added incorrectly, due to adding some of the H atoms to the incorrect copies of those atoms. Hence we must recalculate the force in step 5 if we want to obtain the correct virial and hence the correct pressure.

Besides the force routines, a couple of other files required modification:

1. thermo.f: We modified thermo.f in order to obtain the correct energies for the TIP4P model. In the calculation of the Coulomb energy in the subroutine energy, once again if atom *i* or *j* is a water oxygen, we use the routine findM to find the coordinates of site M, which is then used in the calculation of the Coulomb energy.
2. pppm.f: The calculation of the long-range Coulomb forces by the pppm method required adjustments for site M. In the subroutine pppm, to convert the electric field to a force on atoms required distribution of that force, which acts on site M, back to the corresponding O and H atoms. The formulas all follow from the corresonding calculations in force.f. In the subroutines particle_map and make_rho, we use the location of site M to set up the potential and charge density

fields for the Poisson solver (rather than the location of the water O atoms). Finally, in electric_field we also find site M for the interpolation of grid values to get the electric field acting on the charged atoms.

3. Bookkeeping: the PEO/water force field was added as nonstyle==8, with appropriate changes and calls to the new force field in start.f, input.f, integrate.f, etc.

Results

To verify that the force field was implemented correctly, we did two simulations. A system of 1000 water molecules was created by randomly placing molecules in a box with a density of roughly 1 g/cc. After pushing off with a soft potential, the nonbond interactions were turned on. Interactions were cutoff at 9 Å, the two bonds and one angle were held fixed using SHAKE, and we used a timestep of 1.8 fs. Running in the NPT ensemble at T = 298 K and P = 1 atm, we get an average density of $\rho = 0.998 \pm 0.002$ g/cc, compared to literature values for TIP4P of $\rho = 0.999$ g/cc[1] or $\rho = 1.001$ g/cc[3]. We find an average potential energy per molecule of –9.83 kcal/mol, compared to the literature value of –10.07 kcal/mol[1].

Finally, we did an NVT run to calculate the intermolecular radial distribution functions at 298 K and a density of $\rho = 0.996$ g/cc. These are shown in Fig. 1. The g(r) compare favorably with previous results from the literature[1,3].

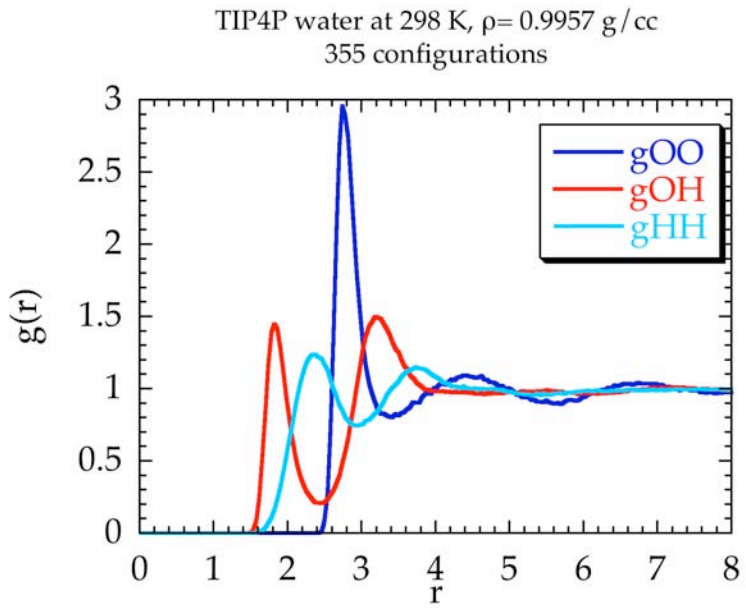

Fig. 1: *Intermolecular correlation function g(r) for TIP4P water (r is in Å).*

References

1. Jorgensen, W.L., et al., *Comparison of simple potential functions for simulating liquid water*. J. Chem. Phys., 1983. **79**(2): p. 926-935.
2. Feenstra, K.A., B. Hess, and H.J.C. Berendsen, *Improving efficiency of large time-scale molecular dynamics simulations of hydrogen-rich systems*. J. Comp. Chem., 1999. **20**(8): p. 786-798.
3. Jorgensen, W.L. and C. Jenson, *Temperature dependence of TIP3P, SPC, and TIP4P water from NPT Monte Carlo simulations: Seeking temperatures of maximum density*. J. Comp. Chem., 1998. **19**(10): p. 1179-1186.

Part 3

The Effect of an Electric Field on the Phase Behavior of a Flory-Huggins Polymer Solution

Consider a polymer solution that we describe by the mean–field, Flory-Huggins theory[1]. The Helmholz free energy of mixing A_0, in the absence of any external fields, is given by[1]

$$A_0 = \frac{\phi \ln \phi}{N} + (1-\phi)\ln(1-\phi) + \chi\phi(1-\phi) \tag{1}$$

where N is the degree of polymerization, ϕ is the volume fraction of polymer and χ is the Flory-Huggins polymer/solvent interaction parameter[1]

$$\chi = \frac{\Delta z \Delta v}{2kT} \tag{2}$$

where $\Delta v = \left(v_{pp} + v_{ss} - 2v_{ps}\right)$. The various $v_{\alpha\beta}$ are the pair attractions between polymer (p) and solvent (s) and z is a coordination number. For van der Waals interactions, it can be demonstrated that χ is always positive. This implies that a polymer solution will phase separate upon cooling. The spinodal curve is determined from the second derivative of the free energy

$$\frac{\partial^2 A_0}{\partial \phi^2} = 0 \tag{3}$$

which leads to the following relationship between χ_S and ϕ_S on the spinodal line

$$\chi_S = \frac{1}{2}\left[\frac{1}{\phi_s N} + \frac{1}{(1-\phi_s)}\right] \tag{4}$$

and a critical point located at $\phi_c = 1/\sqrt{N}$ and $\chi_c = 1/2 + 1/\sqrt{N}$.

We now investigate the question of whether the spinodal curve and critical point shift as a result of the application of a uniform electric field E to the solution. Following the continuum approach of Landau and Lifshitz[2], the Helmholtz free energy in the presence of an electric field can be written as

$$A = A_0 + \frac{\varepsilon_{eff} E^2}{8\pi} \tag{5}$$

where ε_{eff} is the dielectric constant of the polymer/solvent mixture. Landau and Lifshitz showed[2] that for a uniform electric field, ε_{eff} is related to the average dielectric constant $\langle\varepsilon\rangle$ and the mean square fluctuation $\langle\Delta\varepsilon^2\rangle$

$$\varepsilon_{eff} = \langle\varepsilon\rangle - \frac{1}{3}\frac{\langle\Delta\varepsilon^2\rangle}{\langle\varepsilon\rangle} \tag{6}$$

Using eq 3 we can obtain the spinodal condition for the polymer solution in the presence of an electric field from

$$\frac{\partial^2 A}{\partial\phi^2} = \frac{\partial^2 A_0}{\partial\phi^2} + \frac{E^2}{8\pi}\frac{\partial^2\varepsilon_{eff}}{\partial\phi^2} = 0 \tag{7}$$

Since the average dielectric constant $\langle\varepsilon\rangle = \phi\varepsilon_p + (1-\phi)\varepsilon_s$ is a linear function of composition involving the pure component dielectric constants, the only contribution of the field E to the spinodal in eq 7 will arise from the fluctuation term in ε_{eff}.

The mean square fluctuation in the dielectric constant $\langle\Delta\varepsilon^2\rangle$ can be related to the concentration fluctuations of polymer using the Clausius-Mossoti equation[3]

$$\langle\Delta\varepsilon^2\rangle = \frac{\left(\langle\varepsilon\rangle - 1\right)^2\left(\langle\varepsilon\rangle + 2\right)^2}{9}\frac{\langle\Delta\phi^2\rangle}{\langle\phi\rangle^2} \tag{8}$$

where $\langle \phi \rangle$ and $\langle \delta\phi^2 \rangle$ are the average concentration and mean square fluctuation respectively. Thus we observe that the external electric field affects the spindal curve and critical point only through the concentration fluctuations in the polymer solution. From eqs 2,4, 7, and 8 we can now express the shift in the spinodal temperature T_S due to a uniform electric field as

$$\frac{T_S - T_S^0}{T_S^0} = \frac{k_B T_S^0 E^2}{216\varepsilon_0 v} \frac{\partial^2}{\partial \phi^2} \left[\frac{(\langle \phi \rangle - 1)^2 (\langle \phi \rangle + 2)^2}{9\langle \phi \rangle} \frac{\langle \delta\phi^2 \rangle}{\langle \phi \rangle^2} \right] \tag{9}$$

where T_S^0 is the spinodal temperature in the absence of an electric field. From a standard analysis of the fluctuations, it is possible to write the concentration fluctuations in the form

$$\frac{\langle \delta\phi^2 \rangle}{\langle \phi \rangle^2} = \frac{k_B T \kappa}{V} \tag{10}$$

where κ is the osmotic compressibility of polymer and V is the total volume of the system. If we substitute eq 10 into eq 9 we obtain

$$\frac{T_S - T_S^0}{T_S^0} = \frac{k_B T_S^0 E^2}{216\varepsilon_0 v} \frac{\partial^2}{\partial \phi^2} \left[\frac{(\langle \phi \rangle - 1)^2 (\langle \phi \rangle + 2)^2}{9\langle \phi \rangle} \right] \frac{k_B T_S^0 \kappa}{V} \tag{11}$$

Note that the shift in spinodal temperature is very small because the volume V in eq 11 is of macroscopic size. However, as the critical temperature is approached, the osmotic compressibility κ becomes very large. Thus we expect a uniform electric field will have a negligible effect on the phase diagram of a polymer solution, except at the critical point.

Let us now investigate the behavior of the ratio κ/V near the critical point. Consider a polymer in a vacuum solvent. The structure of the polymer in this solution can be computed from PRISM theory[4]. An analytical solution of PRISM theory can be

obtained when the polymer is treated as a thread with a statistical segment length ℓ. Within this approximation we can write the structure factor as

$$\hat{S}(k) = \frac{12(\phi/\ell)^2}{1+(k\xi)^2} \tag{12}$$

where k is the wave vector and ξ is a correlation length for the concentration fluctuations. In the limit of zero wave vector, the structure factor is simply related to the compressibility κ and concentration ϕ of the system

$$\kappa = \frac{\hat{S}(0)}{k_B T \phi} = \frac{12(\phi/\ell)^2}{k_B T \phi} \tag{13}$$

As the critical point is approached the correlation length diverges and ξ^3 becomes comparable the volume V of the system. Thus near the critical point we expect that

$$\frac{\kappa}{V} \sim \frac{12}{k_B T \phi \ell^2} \frac{V^{2/3}}{V} \sim V^{-1/3} \tag{14}$$

Hence, even at the critical point, the shift in spinodal temperature with electric field is small for macroscopic size systems since

$$\frac{T_S - T_S^0}{T_S^0} \sim V^{-1/3} \tag{15}$$

This has indeed been found to be the case in the experiments of Wirtz and Fuller[5] from light scattering experiments on polystyrene solutions in the presence of an electric field. It can be seen from Figure 1 that the maximum shift measured[5] in the critical temperature of a polystyrene/cycolhexane solution was only 0.05 ^{O}C

For many applications it would be desirable to be able to use an electric field to switch a polymer solution between the miscible and immiscible regimes at fixed temperature. Based on the analysis presented here we conclude that a uniform electric

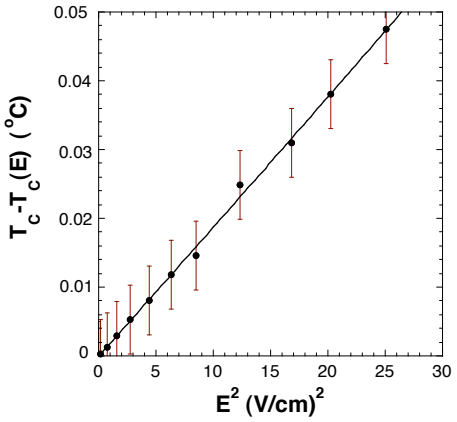

Fig. 1. The shift in critical temperature as a function of the electric field squared measured by Wirtz and Fuller[5] on polystyrene/cyclohexane solutions.

field would not be effective for this purpose. However, recently Tsori et al[6] found that nonuniform electric fields can have a very large effect on the microphase separation of block copolymers. When the field is nonuniform, one the effect does not only depend on the concentration fluctuations, which are small, but also on the average concentration in the solution. Therefore, using nonuniform electric fields seems to be a promising approach for switching polymer solutions. An analysis of nonuniform fields will be the subject of future investigations.

References

1. Flory, P. J.; *Principles of Polymer Chemistry*; Cornell University Press: Ithaca, NY, 1953.
2. Landau, L.; Lifshitz, L., *Electrodynamics of Continuous Media*, Permagon, 2nd Ed., 1984.
3. Callen, H. B.; *Thermodynamics and an Introduction to Thermostatistics,* John Wiley & Sons: New York, 2nd Ed., 1985.
4. Schweizer, K. S.; Curro, J. G.; *Adv. Chem. Phys.* **1997**, *98*, 1.
5. Wirtz, D.; Fuller, G. G.; *Phys. Rev. Lett.* **1993**, 71, 2236.
6. Tsori, Y.; Tournilhac, F.; Leibler, L. *Nature*, **2004**, 430, 544.

Distribution:

6	MS 1349	John G. Curro, 1843
6	MS 1411	Amalie L. Frischknecht, 1834
1	MS 1349	William Hammetter, 1843
1	MS 1411	Eliot Fang, 1834
1	MS 1411	Frank van Swol, 1834
1	MS 1411	Michael S. Kent, 1812
1	MS 1411	Mark J. Stevens, 1834
1	MS 1110	Laura J. D. Frink, 9212
1	MS 1110	Steven J. Plimpton, 9212
1	MS 1415	Gary S. Grest, 1114
1	MS 9108	Central Technical Files, 8945-1
2	MS 0899	Technical Library, 9616
1	MS 0323	LDRD Office, 1011